PERGAMON

International Journal of Heat and Mass Transfer 43 (2000) 1777–1790

International Journal of HEAT and MASS TRANSFER

www.elsevier.com/locate/ijhmt

Experimental balances for the second moments for a buoyant plume and their implication on turbulence modeling

Aamir Shabbir[a,*], Dale B. Taulbee[b]

[a]*Institute for Computational Mechanics in Propulsion, NASA Glenn Research Center, Cleveland, OH 44135, USA*
[b]*State University of New York, Buffalo, NY 14260, USA*

Received 17 July 1998; received in revised form 3 August 1999

Abstract

The experimental budgets for the transport equations for heat flux and Reynolds stress are presented for a round turbulent buoyant plume. The pressure correlation terms are deduced as the closing terms and are found to constitute a substantial part of these budgets. Even though a buoyant plume is initiated by buoyancy, it is found that the production of heat flux and Reynolds stress is largely maintained by the mean flow gradients, because the buoyancy production terms are not as large. The results are used to assess the local equilibrium assumption, which implies that the production and destruction terms of the transport equations balance each other. The results are also used to investigate why the mechanical to thermal time scale ratio for a buoyant plume is different than the commonly used value. Finally, some simpler models for the pressure correlation terms, which appear in the heat flux and the Reynolds stress equations, are assessed against those deduced from the experiment.

Keywords: Buoyant plume; Turbulence models

1. Introduction

The past two decades have seen a tremendous amount of activity toward the second order closure modeling of turbulence. Many (e.g. Launder et al. [1], Lumley [2]) share the view that these models will become the standard tools for the calculation of engineering turbulent flows. Despite their believed importance and large quantity of work published about these models, very little experimental information is available about the budgets of the second moment equations. Part of the problem stems from our inability to measure the pressure correlations. However, if everything else appearing in the transport equations for the second moments is known from the experiment, pressure correlations can be obtained as the closing terms. At present this is the closest we can come to in obtaining these terms from experiment, and despite the measurement errors these balances provide very useful information for the turbulence modelers.

This paper reports the balances for the heat flux and Reynolds stress equations for a round turbulent buoyant plume using the data of Shabbir and George [3]. It is the first time that these budgets are reported for a buoyant plume and therefore this paper adds new in-

* Corresponding author. Tel.: +1-216-433-5927; fax: 991-216-433-8864.
E-mail address: aamir.shabbir@grc.nasa.gov (A. Shabbir).

0017-9310/00/$ - see front matter
PII: S0017-9310(99)00253-7

Nomenclature

b_{ij}	anisotropic tensor
F_0	buoyancy flux
g	gravitational acceleration
p	fluctuating pressure
$\overline{q^2}$	trace of the Reynolds stress tensor
r	radial coordinate
u, v, w	radial, azimuthal and vertical fluctuating velocity components, respectively
U, V, W	radial, azimuthal and vertical mean velocity components, respectively
z	vertical coordinate
Greek symbols	
β	coefficient of thermal expansion
β_i	buoyancy vector, $= (0, 0, -g\beta)$
δ_{ij}	Kronecker delta
ϵ, ϵ_θ	dissipation rates of $\overline{q^2}/2$ and $\overline{\theta^2}/2$
η	the spatial similarity variable
θ, Θ	fluctuating and mean temperature, respectively
Γ	thermal conductivity
ν	kinematic viscosity
τ_r	ratio of the mechanical and thermal time scales
Π_i	sum of the pressure temperature correlation and the molecular destruction term
ρ	density
Φ_{ij}	sum of the pressure strain and anisotropic part of the mechanical dissipation rate tensor.

formation to the existing literature on these flows. The pressure correlation terms are obtained as the closing terms. The balances are used to identify the dominant terms which are responsible for the evolution of heat flux and Reynolds stress in a buoyant plume. The implications of these balances on some of the ideas used in turbulence modeling are discussed. The first of these is the assumption of local equilibrium, which implies that the transport of the Reynolds stresses and the turbulent heat flux is locally balanced between their production and destruction terms. Under such conditions the differential equations can be approximated by the corresponding algebraic equations thus resulting in considerable simplification of the closure problem. The second of these is the the ratio of the mechanical to thermal time scale. A universal value of this parameter would imply that a transport equation for thermal dissipation rate is not required for the closure of equations. Finally, some of the popular models for the pressure correlations are assessed against the experimentally deduced profiles, by assuming that the pressure diffusion is negligible.

2. Turbulent buoyant plume

A buoyant plume is a flow which is initiated and maintained by buoyancy forces. An example is a flow initiated by heating a circular disc. In a laboratory it is difficult to generate a fully developed turbulent flow in this manner and other ways, such as a heated vertical jet, are used to obtain the same flow field. The schematic of the flow and nomenclature is given in Fig. 1. The vertical and radial coordinates are z and r, respectively. The buoyancy vector is designated by $\beta_i = (0, 0, -g\beta)$ where g is the gravitational acceleration in z direction, and β is the coefficient of thermal expansion. The mean vertical velocity is represented by W, the mean radial velocity by U and the mean temperature by Θ. The temperature difference is defined as $\Delta\Theta = \Theta - \Theta_\infty$, where Θ_∞ is the ambient temperature. Turbulence variables are represented by the lower case letters.

This study will use the experimental data of Shabbir and George [3] who generated a buoyant plume by forcing a jet of hot air into an isothermal and quiescent ambient. The details of the experiment are given in the above reference and here we will briefly summarize the essential features of their experiment in

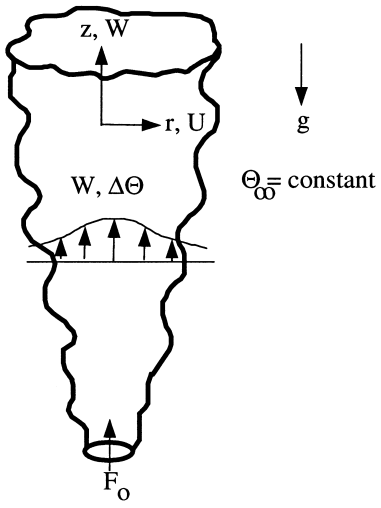

Fig. 1. Schematic of the buoyant plume and the nomenclature.

order to give the reader background for the present paper. The temperature of the air at the source was about 300°C above the ambient. At a distance of about 1 m above the source the centerline flow temperature was of the order of 20°C above the ambient and the mean flow centerline velocity at this location was of the order of 1 m/s. The flow field at a certain distance away from the source (about 0.76 m, which is about 12 times the source nozzle diameter) was characterized by buoyancy forces alone and, therefore, beyond such a location the flow was a laboratory approximation of a turbulent buoyant plume. It should be noted that the buoyancy force in this experiment is characterized by the temperature field.

Batchelor [4] showed that for a turbulent buoyant plume in a neutral environment the equations of motion permit similarity solution. For a round plume the radial profiles of correlations at different vertical locations scale to a single profile if the temperature is scaled by $\Theta_s = F_0^{2/3} z^{-5/3}$, the velocity is scaled by $W_s = F_0^{1/3} z^{-1/3}$, and spatial coordinate is scaled as r/z. In the above relations F_0 is the rate at which buoyancy is added at the source and is given by

$$F_0 = 2\pi \int_0^{r_0} Wg \frac{(\rho_\infty - \rho)}{\rho} r \, dr$$

where ρ is the flow density and ρ_∞ is the ambient density. For a buoyant plume in a neutral environment, as is the case here, F_0 is preserved.

In the experiment of Shabbir and George [3] the instantaneous values of the radial and vertical velocity components and temperature were measured simultaneously at several radial points at various vertical locations using hot-wires. From these measurements various correlations up-to third order were computed. By expressing these correlations in the above similarity variables and fitting them with polynomials, their derivatives in the vertical and radial direction could be computed. It is shown in Ref. [3] that the flow achieved self-similarity over the distances where the measurements were taken. The accuracy of the experiment was checked against the integral constraints as well as by carrying out the balances of the mean momentum and mean energy differential equations. The experiment conserved the buoyancy flux, F_0 within 10%. The thermal dissipation rate, ϵ_θ, and the mechanical dissipation rate, ϵ, were obtained by balancing the transport equations of temperature variance, $\overline{\theta^2}/2$ and the turbulence kinetic energy, $\overline{q^2}/2$ (see Appendix B). It should be pointed out that the pressure diffusion term appearing in the turbulence kinetic energy equation was *estimated* from the model of Lumley [3]. This model approximates the pressure diffusion term as $\partial(\overline{pu_i})/\partial x_i = -(1/5)\partial(\overline{q^2 u_i})/\partial x_i$, where $q^2 = u^2 + v^2 + w^2$ which implies that the pressure diffusion reduces the the turbulent diffusion by 20%. Since diffusion term was not the dominant term in the kinetic energy balance, the approximation of the pressure diffusion was not critical in establishing the level of mechanical dissipation rate.

3. Transport-budget equations

3.1. Transport equations

In this section, we will write and re-arrange the transport equations for the turbulent heat flux and the Reynolds stress for a buoyant plume for their later use in balancing the experimental data. The transport equation for the heat flux $\overline{u_i\theta}$ in tensor notation can be written as

$$U_k(\overline{u_i\theta})_{,k} = -(\overline{u_i u_k \theta})_{,k} - \overline{u_i u_j}\Theta_{,j} - \overline{u_k\theta} U_{i,k} - \beta_i \overline{\theta^2} - \frac{1}{\rho}\overline{\theta(p)_{,i}} - (\nu + \Gamma)\overline{u_{i,k}\theta_{,k}} \quad (1)$$

where a comma has been used to represent spatial derivative; ν is the kinematic viscosity; and Γ is the molecular conductivity. The molecular diffusion term has been neglected since it can be shown to be small as compared to the turbulent diffusion. The term on the left side of Eq. (1) represents advection. The first term on the right side of Eq. (1) represents turbulent diffusion; the second and third terms represent production through mean temperature and mean velocity gradients, respectively. The fourth term represents turbulent buoyancy force and is a production term in general. The first term on the second line of Eq. (1) is the pressure correlation term. The last term represents viscous destruction of the heat flux. This term is thought to get weaker with increasing Reynolds and Peclet numbers, eventually approaching a value of zero in the limit of local (small scale) isotropy. This term was not measured by Shabbir and George [3] and, therefore, its magnitude relative to the other terms can not be established. However, in turbulence modeling, it is customary to combine this term with the pressure correlation term (Lumley [2]). Therefore, from this point of view not knowing each term separately does not reduce the usefulness of the budgets given in this paper. The sum of the pressure correlation and the molecular destruction terms is represented as Π_i in the rest of the paper (i.e. $\Pi_i = -\frac{1}{\rho}\overline{\theta(p)_{,i}} - (\nu + \Gamma)\overline{u_{i,k}\theta_{,k}}$). Measurements reported in Shabbir and George [3] allow the calculation of each of the terms in Eq. (1) except Π_i. Therefore, Π_i is obtained as the closing term in the balance of Eq. (1). (Appendix B estimates the errors involved in deducing Π_i.)

The transport equation for the Reynolds stress $\overline{u_i u_j}$ within the Bussinesq approximation is

$$U_k\left(\overline{u_iu_j}\right)_{,k} = -\left[\overline{u_iu_ju_k}\right]_{,k} - \overline{u_iu_k}U_{j,k} - \overline{u_ju_k}U_{i,k} - \beta_i\overline{u_j\theta} - \beta_j\overline{u_i\theta} + \frac{1}{\rho}\left(\overline{u_ip_{,j} + u_jp_{,i}}\right) - 2\epsilon_{ij} \quad (2)$$

where the viscous diffusion term has been neglected since in this flow it is small compared to the turbulent diffusion. The first term on the right side of Eq. (2) represents turbulent diffusion; the next two terms represent production of the Reynolds stress through the mean velocity gradients. The next two terms represent production of the Reynolds stress by turbulent buoyancy force. Note that these two terms couple the turbulent velocity and temperature fields. The pressure correlation term on the second line is considered responsible for energy transfer between the different components of Reynolds stresses. The last term, ϵ_{ij}, is the viscous dissipation term $\nu\overline{u_{i,k}u_{j,k}}$.

Following Lumley [2] we will rewrite the above equation by adding and subtracting the trace of dissipation term $2\epsilon_{ij}$, which is $(2/3)\epsilon\delta_{ij}$ (δ_{ij} being the Kronecker delta), so that

$$U_k\left(\overline{u_iu_j}\right)_{,k} = -\left[\overline{u_iu_ju_k}\right]_{,k} - \left(\overline{u_iu_k}U_{j,k} + \overline{u_ju_k}U_{i,k}\right) - \beta_i\overline{u_j\theta} - \beta_j\overline{u_i\theta} + \left\{\frac{1}{\rho}\left(\overline{u_ip_{,j} + u_jp_{,i}}\right) - 2\epsilon_{ij} + \frac{2}{3}\epsilon\delta_{ij}\right\} - \frac{2}{3}\epsilon\delta_{ij} \quad (3)$$

Note that in rearranging the above equation the anisotropic part of the dissipation rate, $-2\epsilon_{ij} + (2/3)\epsilon\delta_{ij}$, has been combined with the pressure correlation term. For locally isotropic turbulence the anisotropic part of the dissipation will be zero. It should be pointed out that in the experiment of Shabbir and George [3] ϵ_{ij} was not measured and that was obtained from the balance of the turbulence kinetic energy equation. The term in the curly brackets on the right side of Eq. (3) will be designated by Φ_{ij} and it is this term which has to be modeled to close the Reynolds stress equation. Measurements reported in Shabbir and George [3] allow the calculation of each of the terms in Eq. (3) except Φ_{ij}, and it will be obtained as the closing term in the balance of Reynolds stress. (Appendix B estimates the errors involved in deducing Φ_{ij}.)

3.2. Heat flux budgets

The two non-zero turbulent heat fluxes for the axisymmetric buoyant plume are those in the vertical and radial direction and are represented as $\overline{w\theta}$ and $\overline{u\theta}$, respectively. Using Eq. (1) the transport equation for the vertical heat flux can be written in the cylindrical coordinates as

$$U\frac{\partial\overline{w\theta}}{\partial r} + W\frac{\partial\overline{w\theta}}{\partial z} \approx -\frac{\partial}{\partial z}\left(\overline{ww\theta}\right) - \overline{uw}\frac{\partial}{\partial r}\Delta\Theta - \overline{w^2}\frac{\partial}{\partial z}\Delta\Theta - \overline{u\theta}\frac{\partial W}{\partial r} - \overline{w\theta}\frac{\partial W}{\partial z} + g\beta\overline{\theta^2} - \Pi_z \quad (4)$$

The approximation sign instead of the equality sign has been used since one of the diffusion term $-\frac{1}{r}\frac{\partial}{\partial r}(\overline{ruw\theta})$ has not been included ($\overline{uw\theta}$ correlation from the experiment [3] is not available). The balance of this equation in similarity form is shown in Fig. 2(a). (The similarity form of all the equations whose balances are presented in this paper is given in Appendix A.) The advection term is of the same magnitude as the buoyancy production term over most of the flow field. Near the flow center the production of vertical heat flux is maintained by the mean temperature gradients and the turbulent buoyancy force, $g\beta\overline{\theta^2}$, since the production through velocity gradients is relatively small in this region. However, for $r/z > 0.1$ ($r/z = 0.1$ approximately corresponds to the plume half width), most of the production is maintained by the mean velocity and mean temperature gradients, and the turbulent buoyancy production is only a small fraction of these two. The transport term is the smallest in this balance and, therefore, contributes least to the transport of the vertical heat flux. Since Π_z was not measured, it is obtained as the closing term in this heat flux balance. The shape of this term is very similar to the shape of the vertical heat flux and its magnitude remains large across the flow field.

The equation for the radial heat flux is

$$U\frac{\partial\overline{u\theta}}{\partial r} + W\frac{\partial\overline{u\theta}}{\partial z} \approx -\frac{1}{r}\frac{\partial}{\partial r}\left(\overline{ruu\theta}\right) - \overline{u^2}\frac{\partial}{\partial r}\Delta\Theta - \overline{uw}\frac{\partial}{\partial z}\Delta\Theta - \overline{u\theta}\frac{\partial U}{\partial r} - \overline{w\theta}\frac{\partial U}{\partial z} - \Pi_r \quad (5)$$

Again the approximation sign is used because the diffusion term $-\frac{\partial}{\partial z}(\overline{ruw\theta})$ has not been included. (Note that, based on the thin layer approximation estimate, this term is smaller than the cross-stream diffusion term.) The balance of this equation is shown in Fig. 2(b). Unlike the vertical heat flux balance, the velocity gradient production is extremely small. This is because the radial mean velocity is much smaller than the vertical mean velocity. There is no turbulent buoyancy production in this equation and all the production is therefore maintained by the mean temperature gradients. Advection and diffusion are of smaller magnitude and tend to cancel each other. The term representing the sum of the pressure correlation and the molecular destruction, Π_r, is obtained as the closing term and makes up a substantial part of the budget. Its shape is similar to the radial heat flux. We also note that this

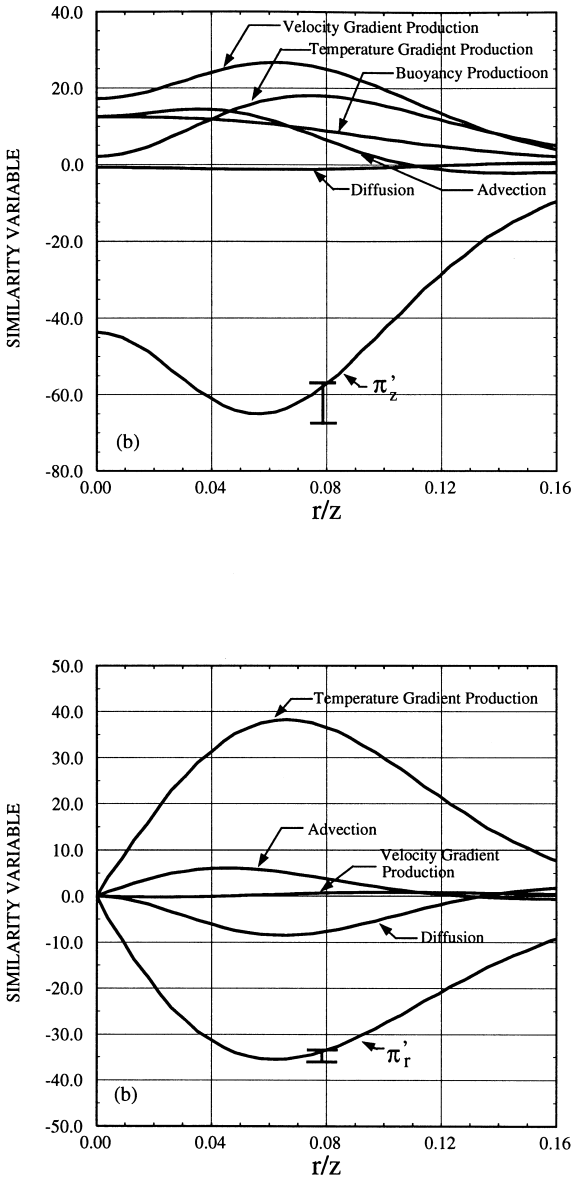

Fig. 2. Experimental budget of the transport equation of (a) vertical heat flux, (b) radial heat flux. The error bars for the pressure correlations are based on the error estimates given in Appendix B.

budget can not be divided into any subregions, where some phenomenon are more dominant than others, because the relative magnitude of each of the terms remains the same across the flow field.

3.3. Reynolds stress budgets

Using Eq. (5) the equation for the Reynolds stress in vertical direction, $\overline{w^2}$, can be written in cylindrical coordinates as

$$U\frac{\partial\overline{w^2}}{\partial r}+W\frac{\partial\overline{w^2}}{\partial z}=-\frac{1}{r}\frac{\partial}{\partial r}\left(r\overline{uw^2}\right)-\frac{\partial}{\partial z}\left(\overline{ww^2}\right)-2\overline{uw}\frac{\partial W}{\partial r}-2\overline{w^2}\frac{\partial W}{\partial z}+2g\beta\overline{w\theta}-\Phi_{zz}-\frac{2}{3}\epsilon \tag{6}$$

The balance of this equation is shown in Fig. 3(a). We notice that the advection is the smallest of all the terms. The diffusion term represents a gain near the center of the plume and a loss elsewhere. Its magnitude near the center is comparable to the other dominant terms in the balance. We note that the turbulent buoyancy production, $2g\beta\overline{w\theta}$, is comparable to the mean gradient production near the plume center but over the rest of the flow field the mean gradient production is much larger than the turbulent buoyancy production. It is interesting to note that the turbulent buoyancy production and dissipation rate approximately balance each other across the flow. The closing term in this balance is Φ_{zz} and represents the sum of the pressure correlation term and the anisotropic part of the dissipation. This term represents a loss for the $\overline{u^2}$ budget and we note that beyond $r/z = 0.08$ this term and the gradient production term approximately balance each other.

The equation for the radial component of the Reynolds stress, $\overline{u^2}$, is given by

$$U\frac{\partial\overline{u^2}}{\partial r}+W\frac{\partial\overline{u^2}}{\partial z}=-\frac{1}{r}\frac{\partial}{\partial r}\left(r\overline{uu^2}\right)-\frac{\partial}{\partial z}\left(\overline{wu^2}\right)-2\overline{u^2}\frac{\partial U}{\partial r}-2\overline{uw}\frac{\partial U}{\partial z}-\Phi_{rr}-\frac{2}{3}\epsilon \tag{7}$$

and its balance is shown in Fig. 3(b). Obviously the advection of $\overline{u^2}$ has the same shape as the advection of $\overline{w^2}$ which was shown earlier. The mean gradient production is a loss near the plume center and is a gain after about $r/z = 0.04$. This is because $\partial U/\partial r$ is positive near the plume center but negative elsewhere. Unlike the $\overline{w^2}$ budget, the gradient production term is not large. The diffusion term is a loss over most of the flow field and becomes a gain toward the outer edge of the flow field. The sum of the pressure correlation term and the anisotropic part of the dissipation rate, Φ_{rr}, is obtained as the closing term in the budget and represents a gain for $\overline{u^2}$. We further note that beyond $r/z = 0.08$ it approximately balances the dissipation rate.

Finally, we look at the budget for the shear stress,

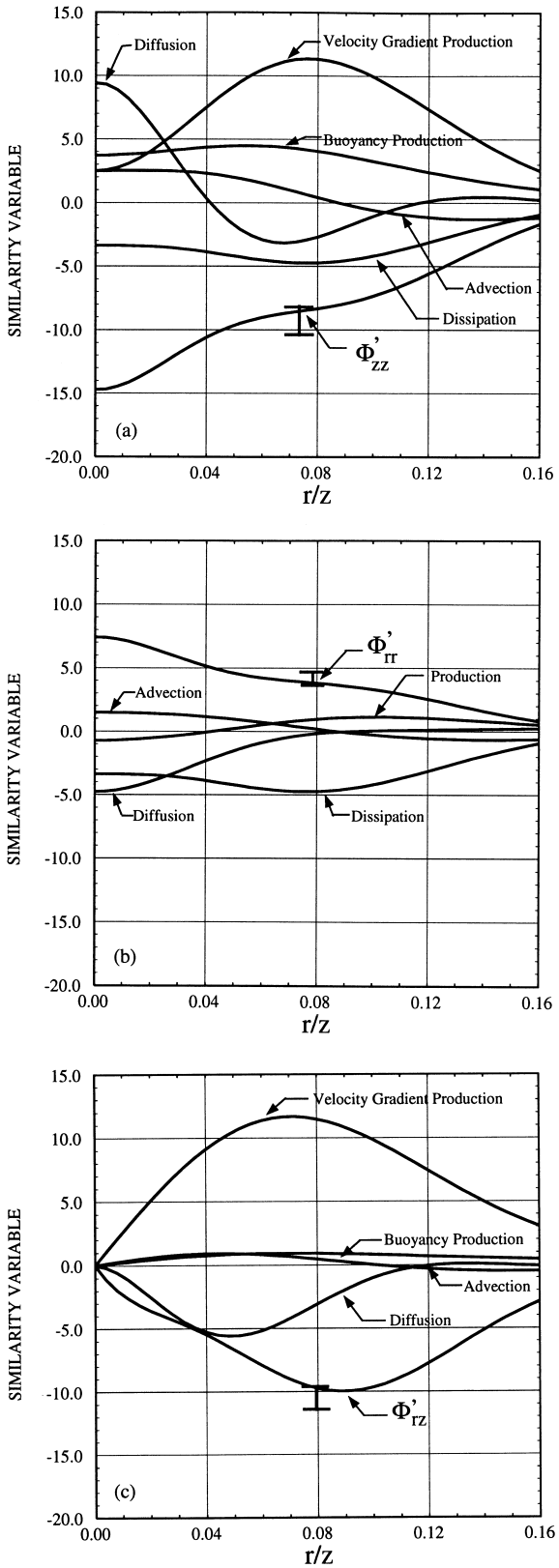

Fig. 3. Experimental budget of the Reynolds stress transport equation. (a) $\overline{w^2}$, (b) $\overline{u^2}$, (c) $\overline{uw}$. The error bars for the pressure correlations are based on the error estimateds given in Appendix B.

$\overline{uw}$, which is represented by the following equation

$$U\frac{\partial \overline{uw}}{\partial r} + W\frac{\partial \overline{uw}}{\partial z} = -\frac{1}{r}\frac{\partial}{\partial r}(r\overline{uuw}) - \frac{\partial}{\partial z}(\overline{wuw}) - \overline{uw}\frac{\partial U}{\partial r} - \overline{w^2}\frac{\partial U}{\partial z} - \overline{u^2}\frac{\partial W}{\partial r} - \overline{uw}\frac{\partial W}{\partial z} + g\beta\overline{u\theta} - \Phi_{rz} \quad (8)$$

and is shown in Fig. 3(c). We note that both the advection and the turbulent buoyancy production are of very small magnitude. Neglecting these two terms would not cause any significant change in the shear stress balance. We note that the diffusion term is not negligible in this budget. The term Φ_{rz} is essentially balanced by the difference between the shear production and the diffusion processes. The shape of Φ_{rz} is similar to that of the shear stress and its peak approximately corresponds to the peak in the shear production.

4. Implications on modeling

4.1. Local equilibrium assumption

The assumption of local equilibrium implies that the evolution of the turbulence is slow enough to ignore the effects of advection and diffusion (or that these two phenomenon balance each other). For the turbulence kinetic energy equation it means that the production and dissipation rates balance each other whereas for the heat flux and Reynolds stress equations it implies that the sum of the production and pressure correlation terms balances the respective molecular destruction terms. This idea forms the basis of the classical algebraic stress models where algebraic expressions for the heat flux and Reynolds stress are obtained by neglecting the above mentioned terms from their differential equations (Rodi [5]). We will use the balances shown in the last section to assess the validity of this assumption.

From the budget of vertical heat flux, Fig. 2(a), it is obvious that the advection and diffusion terms are small and ignoring these will have no effect on the heat flux. In the radial heat flux budget, Fig. 2(b), the advection and diffusion terms approximately balance each other. One can argue that the neglect of these two terms will introduce an error which is within the other approximations used in the algebraic stress

models. Therefore, it seems that for the heat fluxes the algebraic models can provide a reasonably good approximation. However, success of these models will depend on the accuracy of the closure expressions for the pressure temperature-gradient correlation. We will look at models for these correlations later in the paper.

On the other hand local equilibrium assumption does not seem to be a good assumption for Reynolds stresses. From the balances of radial and shear stress components (Fig. 3(b) and (c)) it is clear that the sum of the advection and diffusion terms is not small and can not be neglected without introducing a large error. This is specially true near the plume center. So we conclude that in a buoyant plume the assumption of local equilibrium is not a good approximation for the Reynolds stresses. This will also be evident when we look at the ratio of mechanical to thermal time scale in the next section.

4.2. Ratio of mechanical to thermal time scales

The time scales $\overline{q^2}/\epsilon$ and $\overline{\theta^2}/\epsilon\theta$ represent the eddy turn over times for the mechanical and thermal fields, respectively and their ratio is widely used in turbulence models. A universal value of the time scale ratio would imply that a transport equation for the thermal dissipation rate is not needed, although it is now realized that this ratio can widely vary from one flow to another and that a better approach would be to use a transport equation (see e.g. Newman et al. [6]).

The time-scale ratio $\tau_r = \overline{q^2}\epsilon_\theta/\overline{\theta^2}\epsilon$ is calculated using the data of Shabbir and George [3] and is found to be 3.3 over most of the flow field. (This value starts to sharply increase as the outer edge of the plume is approached. The measurement errors are quite large at this location and it is not clear whether this rise is due to the measurement errors alone or also because the mechanical dissipation rate approaches zero faster than the thermal dissipation rate.) Note that Appendix B gives estimates of errors involved in calculating the two dissipation rates. Using these errors it is found that the time scale ratio is underestimated by 8%. This error is smaller than what one might have expected because the two dissipation rates occur as a ratio in the definition of time scale ratio, and as a result the errors compensate each other.

This value is substantially different than the commonly used value of 2.0 which was recommended by Beguier et. al. [7] after analyzing experiments on wall bounded (turbulent flat plate boundary layer, and fully developed pipe flow) and boundary free shear flows (heated wake, and mixing layer). The dissipation rates were not available for some of these experiments and were obtained by invoking the local equilibrium assumption. The authors further noted that the turbulence was found to be in local equilibrium for near wall flows and that although this was not true for the free shear flows, the production and dissipation rates were still the dominant processes for these flows as well. In the present experiment the production and dissipation processes are certainly the dominant ones but advection and transport are large enough so that the local equilibrium assumption is not satisfied for the $\overline{q^2}$ and $\overline{\theta^2}$ equations. This is the reason that the value of time scale ratio for a buoyant plume differs from that obtained by Beguier et al. [7]. This can be further illustrated by calculating the time scale ratio by using the local equilibrium assumption. With this assumption the mechanical and thermal dissipation rates, which are needed for computing the time scale ratio, are calculated from the following expressions

$$\epsilon = -\overline{u_i u_j} U_{i,j} - \beta_i \overline{u_i \theta}$$

$$\epsilon_\theta = -\overline{u_i \theta} \Theta_{,i}$$

as opposed to deducing them from the transport equations for turbulence kinetic energy and turbulence thermal variance. Interestingly enough the time scale ratio obtained with these approximation is about 2.0 across most of the flow field.

It is of interest to compare the results of the buoyant plume with the experiment of Tavoularis and Corrsin [12], where homogeneous turbulence was subjected to constant cross-stream mean velocity and temperature gradients. The time scale ratio for their experiment is about 3.0 which coincidently is close to what is found here for the buoyant plume. If local equilibrium assumption is used to calculate the time scale ratio r for the experiment of Tavoularis and Corrsin [12], then surprisingly its value comes to about 2.0. It should be noted that the buoyancy effects are absent in their experiment and that the temperature behaves as a passive scalar. The similarities between the time scale ratios for the two experiments could be due to the fact that the relative magnitudes of the production and dissipation rates are similar in these experiments. It should be emphasized that the purpose of this comparison is not to advocate a new universal value of the time scale ratio but only to show that the use of local equilibrium assumption in calculating the time scale ratio can result in large errors.

4.3. Assessment of models for the pressure correlation term in the heat flux equation

At second order closure level the pressure correlation terms in the turbulent heat flux and Reynolds stress equations have to be modeled. In this section, we will compare two of the simpler models for these

correlations with those obtained from the experimental budgets by assuming that the pressure diffusion term is small and can be ignored.

In turbulence modeling the pressure correlation term in the heat flux term is rewritten in the following manner

$$\frac{1}{\rho}\overline{\theta(p)}_{,i} = \frac{1}{\rho}\left(\overline{p\theta}\right)_{,i} - \frac{1}{\rho}\overline{p(\theta)}_{,i}$$

where the first term on the right side is a diffusion like term and tends to redistribute the heat flux where as the second term on the right side is a source/sink term for the heat flux. Based on the above splitting we can write Π_i as

$$\Pi_i = \frac{1}{\rho}\left(\overline{p\theta}\right)_{,i} - \frac{1}{\rho}\overline{p(\theta)_i} - (\nu + \Gamma)\overline{u_{i,j}\theta_{,j}}$$

$$= \frac{1}{\rho}\left(\overline{p\theta}\right)_{,i} + \Pi_i' \tag{9}$$

where the definition of Π_i' is obvious. Lumley [2] has proposed that the diffusion term can be modeled as $(\overline{p\theta})_{,i}/\rho = (1/5)(\overline{u_k u_k \theta})_{,i}$. Most of the other modelers ignore the pressure diffusion term with the view that at least for the boundary free shear flows the magnitude of this term is small as compared to the other terms in the equation. For the present flow we can at best make an estimate of this term using the above model. We find that at most the Π_i will be reduced by 13%. So neglecting the pressure diffusion is a reasonable approximation for this flow. Therefore, we will assume that $\Pi_i \approx \Pi_i'$ for the present flow.

Now we will list the two models for Π_i and then compare them with the experiment. The first one is taken from Launder [13] and is represented by the following equation.

$$\Pi_i = -C_{1\theta}\frac{\epsilon}{k}\overline{u_i\theta} - C_{2\theta}\overline{u_j\theta}U_{i,j} + C_{3\theta}\beta_i\overline{\theta^2} \tag{10}$$

The first term represents the model for the slow part and was originally proposed by Monin [9]; the second term represents the model for the rapid part; and the third term represents the model for the buoyancy part. The model constants are: $C_{1\theta} = 3.0$, $C_{2\theta} = 0.5$, and $C_{3\theta} = 0.5$.

The second model to be considered here is due to Zeman and Lumley [10] and is given by

$$\Pi_i = -(\tau_r + C_1)\frac{k}{\epsilon}\overline{u_i\theta} - \frac{4}{5}U_{l,m}\left(\delta_{li}\overline{u_m\theta} - \frac{1}{4}\delta_{mi}\overline{u_l\theta}\right) + \frac{1}{3}\beta_i\overline{\theta^2} \tag{11}$$

We note that the form of both the slow and the buoyancy parts in this model is the same as that in model (10). However, the slow term coefficient is not assigned a constant value in this model but instead is a function of the time scale ratio τ_r and the anisotropy invariants. The coefficient C_1 is given by [8]

$$C_1 = \frac{1.}{(-15.*\Pi)}\left[1. + (1. - 24.*\Pi)^{1/2}\right]$$

$$\Pi = b_{ij}b_{ij}$$

$$b_{ij} = \frac{\overline{u_i u_j}}{\overline{q^2}} - \frac{1}{3}\delta_{ij} \tag{12}$$

The right side of models (10) and (11) can be directly calculated from the experimental data reported by Shabbir and George [3]. This can then be compared to the pressure correlations presented earlier in this paper. The results from model (10) for the Π_z correlation are compared with the experiment in Fig. 4(a), where each of the three terms constituting Π_z model are also plotted. We note that the model under-predicts the experiment, with the model peak at about 50% of the experiment. Fig. 4(b) shows the similar comparison for Π_r component. The buoyancy part of this component is zero and the total modeled correlation for Π_r is the sum of the slow and the rapid parts. We further note that the rapid part is extremely small and all of the modeled Π_r correlation is thus represented by the slow part. The peak level of model is about 25% of the experiment. We note that the the shapes of both Π_z and Π_r from the model are similar to the experiment. Obviously, there are errors involved in deducing Π_i from the experimental data (see Appendix B) and in ignoring the pressure diffusion. However, the differences between model and the experiment in the above comparisons is so large that it can not be explained by these errors.

Fig. 5 represents the results from model (11). We note that Π_z from the model agrees very well with the experiment since the differences in the two are certainly within the experimental error. We note that the improved performance of this model over model Eq. (10) is due to larger values of both slow and rapid terms. Fig. 5(b) shows the results for Π_r. For this component the buoyancy part of the model is zero and the Π_r correlation is represented by the sum of slow and rapid parts. We note that, unlike model (10), the sign of the rapid term is opposite to that of the slow term and the sum of the two greatly under-predicts the experiment, with the peak value from the model at about 20% of the experiment. This discrepancy is much larger than the experimental error in Π_r which is discussed in Appendix B. It should be pointed out that in shear dominated flows, such as boundary free shear flows and boundary layers, it is more important to predict the cross-stream heat flux correctly than the

stream-wise heat flux. Apparently, Zeman and Lumley [10] were aware of this shortcoming of their model as they, on ad-hoc basis, changed the sign of the rapid part of their model in order to obtain better agreement between their computation and the experimental data on planetary boundary layers (Zeman [11]).

It is also useful to carry out a similar comparison for the above models with the homogeneous shear flow experiment of Tavoularis and Corrsin [12] to see if the comparisons with the buoyant plume represent an anomaly. For this experiment Π_x and Π_y represent the stream-wise and the cross-stream components of pressure correlation, respectively, and the pressure diffusion term is zero. Furthermore, the pressure correlation consists of only the slow and rapid parts. The experimental value of the pressure correlation, which was obtained from the balance of the heat flux equations [6], is compared with the model Eqs. (10) and (11) in Table 1. We notice similar trends for this flow as we did for the plume. Both the models under-predict the

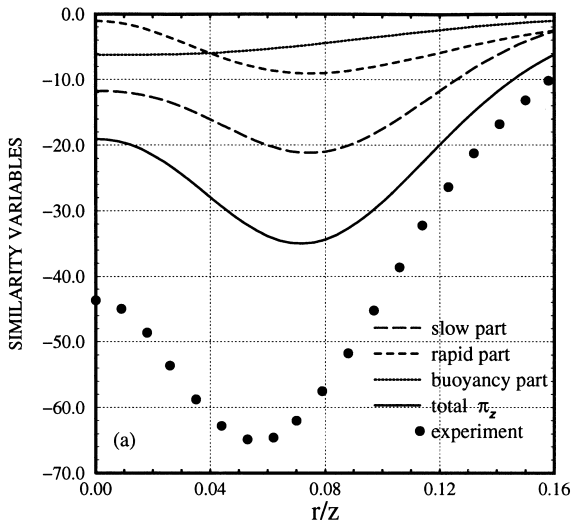

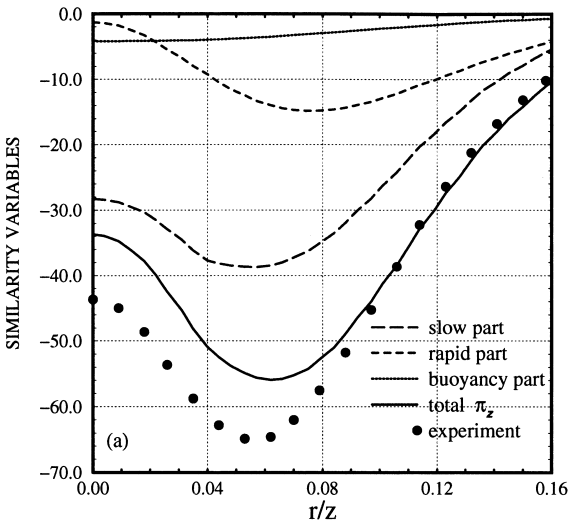

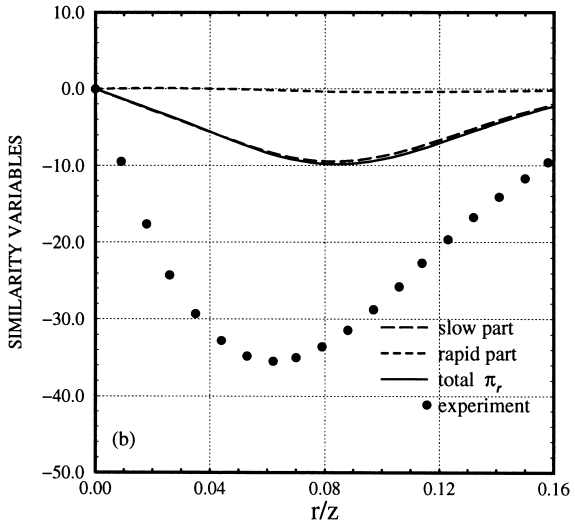

Fig. 4. Comparision of the Launder (1975) model of the pressure–temperature correlation with its experimentally deduced profile. (a) π_z component. (b) π_r component.

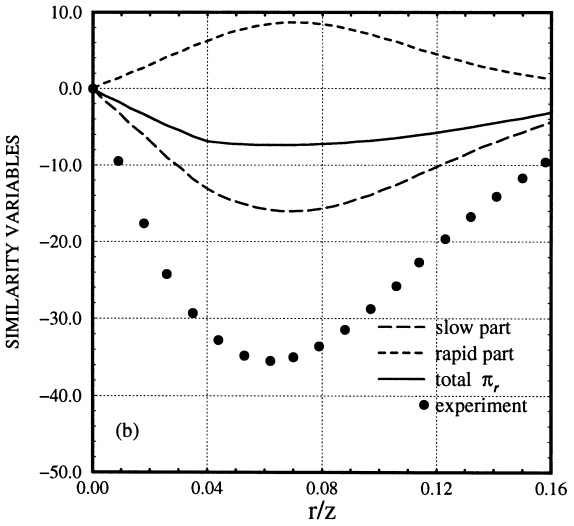

Fig. 5. Comparison of the Zeman and Lumley (1976) model of the pressure–temperature correlation with its experimentally deduced profile. (a) π_z component and (b) π_r component.

Table 1
Comparison between the experiment of Tavoularis and Corrsin and models for Π_i

$x/H = 11.0$	Slow part of Π_y	Rapid part of Π_y	Total Π_y	Slow part of Π_x	Rapid part of Π_x	Total Π_x
Experiment	–	–	1.412	–	–	−1.909
Zeman–Lumley	0.798	−0.472	0.326	−1.809	−0.833	−2.642
Launder	0.541	0.000	0.541	−1.227	−0.520	−1.747

experiment. Furthermore, the sign of the rapid part of the cross-stream pressure correlation, Π_y, is opposite to the slow part, Π_y, for model Eq. (11).

From these comparisons we conclude that the model for the pressure correlation are defective and need to be improved. Furthermore, any algebraic stress models obtained from these second order models will be deficient not because the local equilibrium assumption is not satisfied for the heat flux transport equation, but because of the deficiencies in the pressure correlation models.

4.4. Models for pressure correlation terms in the Reynolds stress equations

The pressure correlation term in the Reynolds stress equations is also split into a pressure–strain correlation term and a pressure diffusion liketerm. Then these two parts are modeled separately. Unlike the heat flux equation, the situation is more subtle for the Reynolds stress equation because Lumley [8] has shown that the splitting of pressure correlation for Reynolds stress equation is not unique (also see Zeman [11]). We will neglect the pressure diffusion term in the comparisons shown below. This implies that we are assuming $\Phi_{ij} \approx \Phi'_{ij}$, where the two are related by

$$\Phi_{ij} = \Phi'_{ij} + \Phi_{ij}^{\text{diffusion}}, \tag{13}$$

$\Phi_{ij}^{\text{diffusion}}$ being the pressure diffusion term.

Several models for Φ_{ij} have been proposed and the reader is referred to several of the review papers which exist in literature [2]. In this study, we will only assess one model which is simpler and is used commonly: the LRR model of Launder et al. [1]. Like its counterpart model for the pressure–temperature gradient correlation, it consists of three parts: the slow part; the rapid part; and the buoyancy part. In Launder et al. [1] only the model for the slow and rapid parts was presented. Therefore, the model for the buoyancy part is taken from Launder [13]. The complete model is given by the following equation.

$$\Phi_{ij} = -C_1\epsilon\left(\frac{\overline{u_iu_j}}{k} - \frac{2}{3}\delta_{ij}\right) - \frac{(c'_2+8)}{11}\left(P_{ij} - 23P\delta_{ij} - \frac{(30c'_2-2)}{55}k\left(U_{i,j}+U_{j,i}\right)\right) - \frac{(c'_2-2)}{11}\left(D_{ij} - \frac{2}{3}P\delta_{ij}\right) - C_3\left(\beta_i\overline{uj t} + \beta_j\overline{u_i t}\right) - \frac{2}{3}\beta_k\overline{u_k t} \tag{14}$$

where $P_{ij} = -\overline{u_iu_k}U_{i,j} - \overline{u_ju_k}U_{j,k}$, $D_{ij} = -\overline{u_iu_k}U_{k,i} - \overline{u_ju_k}U_{k,j}$ and $P = P_{ii}$. The model constant c'_2 of the LRR model has evolved to slightly different value than that originally recommended by LRR [1]. Using new experiments on homogeneous shear flow a more accurate calibration has been carried out by several authors (see Morris [14] and Taulbee et al. [15]). The values of constants used in the present study are: $C_1 = 1.8$ and $c'_2 = 0.55$.)

The results are shown in Fig. 6. For the Φ_{zz} component we note that there is a large discrepancy between the experiment and the model near the centerline. For the rest of the flow region we note that the model level is slightly more negative than the experiment although the difference here lies within the experimental uncertainty. Similar conclusions can be drawn for the Φ_{rr} comparisons shown in Fig. 6(b). The comparison for the Φ_{rz}, which is the most important component, is shown in Fig. 6(c) and we note that both the shape and the level of the model is in reasonable agreement with the experimentally deduced profile, and the differences between the two could be due to the experimental errors and the neglect of pressure diffusion.

5. Summary and conclusions

The balances for the heat flux and Reynolds stresses were presented for a round turbulent buoyant plume using the experimental data of Shabbir and George [3]. These provide useful information about the relative magnitude of the different terms in the heat flux and Reynolds stress equations. The pressure correlation terms were deduced as the closing terms in these equations. It was found out that these terms represent a substantial part of these budgets. The turbulent

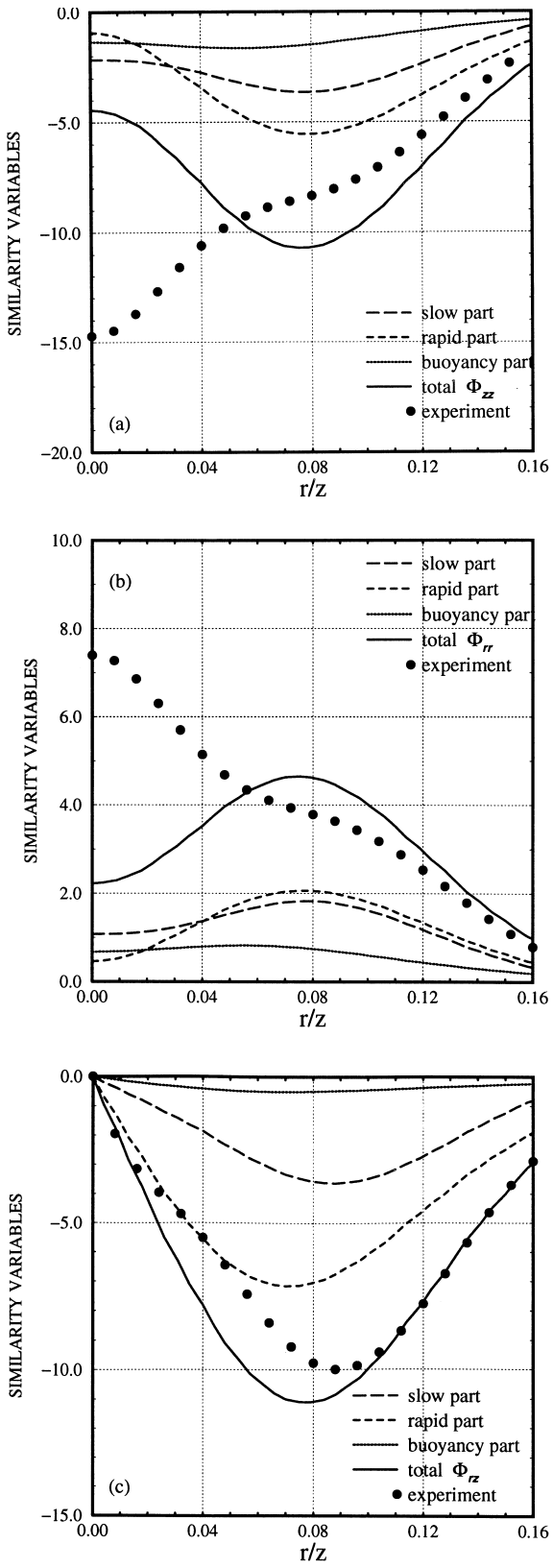

Fig. 6. Comparison of the model of the pressure–strain correlation with its experimentally deduced profile. (a) Φ_{zz} component, (b) Φ_{rr} component, and (c) Φ_{rz} component.

buoyancy force was substantial for the vertical heat flux and vertical Reynolds stress budgets only, but even then most of the production was due to the mean flow gradients. Therefore, it is concluded that for a buoyant plume the heat flux and Reynolds stresses are largely maintained by the mean flow gradients.

These balances were used to assess the assumption of local equilibrium which forms the basis for the classical algebraic stress models. It is found that the local equilibrium assumption is a reasonable approximation for the heat flux transport equation. However, it is not a good assumption for the Reynolds stress transport equation because the sum of the advection and diffusion terms can not be ignored. It was also investigated as to why the time scale ratio for a buoyant plume, which has an average value of 3.3 across the flow, is different than the commonly used value of 2.0. It was found that this difference is a consequence of the local equilibrium assumption not being satisfied for the buoyant plume.

Finally, some of the simpler models for the pressure correlation terms, which appear in the transport equations for the heat flux and Reynolds stress, were compared with the experimentally deduced profiles. In making these comparisons it was assumed that the pressure diffusion is small and can be ignored. It was found that the models for the pressure correlations greatly under-predict the data and the possibility of deficiency in the rapid term model was pointed out. These models need to be improved before they can be used for accurate predictions for such flows. On the other hand the model for the pressure strain term, which appears in Reynolds stress transport equation, showed a reasonable agreement with its experimentally deduced profile. Finally, we note that these conclusions apply only to the buoyant plume flow and can not be generalized to other flows. After similar comparisons have been made with several other flows, only then can a general assessment of these model can be made.

Appendix A

Here we give the similarity form of the heat flux and Reynolds stress equations for a round buoyant plume in a neutral environment. These equations are applicable in a fully developed region where the flow is self similar. The spatial similarity variable is $\eta = r/z$. We have made use of the relations $\frac{\partial}{\partial r} = (1/z)\frac{\mathrm{d}}{\mathrm{d}\eta}$ and $\frac{\partial}{\partial z} = (-\eta/z^2)\frac{\mathrm{d}}{\mathrm{d}\eta}$ which are obtained by using the chain rule of differentiation. In the following equations every quantity enclosed in the square brackets is a function

of η only and represents asimilarity variable. The following equations are written out in such a way so that the reader can easily recognize the corresponding terms in the non-similarity form of the equations.

$$\begin{aligned}
&\left[UF_0^{-1/3}z^{1/3}\right]\frac{\mathrm{d}}{\mathrm{d}\eta}\left[\overline{w\theta}g\beta F_0^{-1}z^2\right]+\left[WF_0^{-1/3}z^{1/3}\right]\Big\{\\
&\quad -2\left[\overline{w\theta}g\beta F_0^{-1}z^2\right]-\eta\frac{\mathrm{d}}{\mathrm{d}\eta}\left[\overline{w\theta}g\beta F_0^{-1}z^2\right]\Big\}\\
&\approx -\left\{\left(\frac{-7}{3}\right)\left[\overline{ww\theta}g\beta F_0^{-4/3}z^{7/3}\right]\right.\\
&\quad \left.-\eta\frac{\mathrm{d}}{\mathrm{d}\eta}\left[\overline{ww\theta}g\beta F_0^{-4/3}z^{7/3}\right]\right\}\\
&\quad -\left[\overline{uw}F_0^{2/3}z^{-2/3}\right]\frac{\mathrm{d}}{\mathrm{d}\eta}\left[\Delta\Theta g\beta F_0^{-2/3}z^{5/3}\right]\\
&\quad -\left[\overline{w^2}F_0^{2/3}z^{-2/3}\right]\left\{\left(\frac{-5}{3}\right)\left[\Delta\Theta g\beta F_0^{-2/3}z^{5/3}\right]\right.\\
&\quad \left.-\eta\frac{\mathrm{d}}{\mathrm{d}\eta}\left[\Delta\Theta g\beta F_0^{-2/3}z^{5/3}\right]\right\}\\
&\quad -\left[\overline{u\theta}g\beta F_0^{-1}z^2\right]\frac{\mathrm{d}}{\mathrm{d}\eta}\left[WF_0^{-1/3}z^{1/3}\right]\\
&\quad -\left[\overline{w\theta}g\beta F_0^{-1}z^2\right]\left\{\left(\frac{-1}{3}\right)\left[WF_0^{-1/3}z^{1/3}\right]\right.\\
&\quad \left.-\eta\frac{\mathrm{d}}{\mathrm{d}\eta}\left[WF_0^{-1/3}z^{1/3}\right]\right\}\\
&\quad +\left[g\beta\overline{\theta^2}g\beta F_0^{-4/3}z^{10/3}\right]-\left[\Pi_z g\beta F_0^{-4/3}z^{10/3}\right] \qquad \text{(A1)}\\
&\left[UF_0^{-1/3}z^{1/3}\right]\frac{\mathrm{d}}{\mathrm{d}\eta}\left[\overline{u\theta}g\beta F_0^{-1}z^2\right]+\left[WF_0^{-1/3}z^{1/3}\right]\Big\{\\
&\quad -2\left[\overline{u\theta}g\beta F_0^{-1}z^2\right]-\eta\frac{\mathrm{d}}{\mathrm{d}\eta}\left[\overline{u\theta}g\beta F_0^{-1}z^2\right]\Big\}\\
&\approx -\frac{1}{\eta}\frac{\mathrm{d}}{\mathrm{d}\eta}\left[\eta\overline{uu\theta}F_0^{-4/3}z^{7/3}\right]\\
&\quad -\left[\overline{u^2}F_0^{2/3}z^{-2/3}\right]\frac{\mathrm{d}}{\mathrm{d}\eta}\left[\Delta\Theta g\beta F_0^{-2/3}z^{5/3}\right]\\
&\quad -\left[\overline{uw}F_0^{2/3}z^{-2/3}\right]\left\{\left(\frac{-5}{3}\right)\left[\Delta\Theta g\beta F_0^{-2/3}z^{5/3}\right]\right.\\
&\quad \left.-\eta\frac{\mathrm{d}}{\mathrm{d}\eta}\left[\Delta\Theta g\beta F_0^{-2/3}z^{5/3}\right]\right\}\\
&\quad -\left[\overline{u\theta}g\beta F_0^{-1}z^2\right]\frac{\mathrm{d}}{\mathrm{d}\eta}\left[UF_0^{-1/3}z^{1/3}\right]\\
&\quad -\left[\overline{w\theta}g\beta F_0^{-1}z^2\right]\left\{\left(\frac{-1}{3}\right)\left[UF_0^{-1/3}z^{1/3}\right]\right.\\
&\quad \left.-\eta\frac{\mathrm{d}}{\mathrm{d}\eta}\left[UF_0^{-1/3}z^{1/3}\right]\right\}\\
&\quad -\left[\Pi_r g\beta F_0^{-4/3}z^{10/3}\right] \qquad \text{(A2)}\\
&\left[UF_0^{-1/3}z^{1/3}\right]\frac{\mathrm{d}}{\mathrm{d}\eta}\left[\overline{w^2}g\beta F_0^{-2/3}z^{2/3}\right]\\
&\quad +\left[WF_0^{-1/3}z^{1/3}\right]\left\{\left(\frac{-2}{3}\right)\left[\overline{w^2}g\beta F_0^{-2/3}z^{2/3}\right]\right.\\
&\quad \left.-\eta\frac{\mathrm{d}}{\mathrm{d}\eta}\left[\overline{w^2}F_0^{-2/3}z^{2/3}\right]\right\}\\
&= -\frac{1}{\eta}\frac{\mathrm{d}}{\mathrm{d}\eta}\left[\eta\overline{uw^2}F_0^{-1}z\right]-\left\{(-1)\left[\overline{ww^2}F_0^{-1}z\right]\right.\\
&\quad \left.-\eta\frac{\mathrm{d}}{\mathrm{d}\eta}\left[\overline{ww^2}F_0^{-1}z\right]\right\}\\
&\quad -2\left[\overline{uw}F_0^{-2/3}z^{2/3}\right]\frac{\mathrm{d}}{\mathrm{d}\eta}\left[WF_0^{-1/3}z^{1/3}\right]\\
&\quad -2\left[\overline{w^2}F_0^{-2/3}z^{2/3}\right]\left\{\left(\frac{-1}{3}\right)\left[WF_0^{-1/3}z^{1/3}\right]\right.\\
&\quad \left.-\eta\frac{\mathrm{d}}{\mathrm{d}\eta}\left[WF_0^{-1/3}z^{1/3}\right]\right\}\\
&\quad +2\left[g\beta\overline{w\theta}F_0^{-1}z^2\right]-\left[\Phi_{zz}F_0^{-1}z^2\right]-\frac{2}{3}\left[\epsilon F_0^{-1}z^2\right] \qquad \text{(A3)}
\end{aligned}$$

$$\left[UF_0^{-1/3}z^{1/3}\right]\frac{\mathrm{d}}{\mathrm{d}\eta}\left[\overline{u^2}g\beta F_0^{-2/3}z^{2/3}\right]$$
$$+\left[WF_0^{-1/3}z^{1/3}\right]\left\{\left(\frac{-2}{3}\right)\left[\overline{u^2}g\beta F_0^{-2/3}z^{2/3}\right]$$
$$-\eta\frac{\mathrm{d}}{\mathrm{d}\eta}\left[\overline{u^2}F_0^{-2/3}z^{2/3}\right]\right\}$$
$$=-\frac{1}{\eta}\frac{\mathrm{d}}{\mathrm{d}\eta}\left[\eta\overline{uu^2}F_0^{-1}z\right]-\left\{(-1)\left[\overline{wu^2}F_0^{-1}z\right]\right.$$
$$\left.-\eta\frac{\mathrm{d}}{\mathrm{d}\eta}\left[\overline{wu^2}F_0^{-1}z\right]\right\}$$
$$-2\left[\overline{u^2}F_0^{-2/3}z^{2/3}\right]\frac{\mathrm{d}}{\mathrm{d}\eta}\left[UF_0^{-1/3}z^{1/3}\right]$$
$$-2\left[\overline{uw}F_0^{-2/3}z^{2/3}\right]\left\{\left(\frac{-1}{3}\right)\left[UF_0^{-1/3}z^{1/3}\right]\right.$$
$$\left.-\eta\frac{\mathrm{d}}{\mathrm{d}\eta}\left[WF_0^{-1/3}z^{1/3}\right]\right\}$$
$$-\left[\Phi_{rr}F_0^{-1}z^2\right]-\frac{2}{3}\left[\epsilon F_0^{-1}z^2\right] \quad \text{(A4)}$$

$$\left[UF_0^{-1/3}z^{1/3}\right]\frac{\mathrm{d}}{\mathrm{d}\eta}\left[\overline{uw}g\beta F_0^{-2/3}z^{2/3}\right]$$
$$+\left[WF_0^{-1/3}z^{1/3}\right]\left\{\left(\frac{-2}{3}\right)\left[\overline{uw}g\beta F_0^{-2/3}z^{2/3}\right]\right.$$
$$\left.-\eta\frac{\mathrm{d}}{\mathrm{d}\eta}\left[\overline{uw}F_0^{-2/3}z^{2/3}\right]\right\}$$
$$=-\frac{1}{\eta}\frac{\mathrm{d}}{\mathrm{d}\eta}\left[\eta\overline{uuw}F_0^{-1}z\right]-\left\{(-1)\left[\overline{wuw}F_0^{-1}z\right]\right.$$
$$\left.-\eta\frac{\mathrm{d}}{\mathrm{d}\eta}\left[\overline{wuw}F_0^{-1}z\right]\right\}-\left[\overline{uw}F_0^{-2/3}z^{2/3}\right]\frac{\mathrm{d}}{\mathrm{d}\eta}\left[UF_0^{-1/3}z^{1/3}\right]$$
$$-\left[\overline{w^2}F_0^{-2/3}z^{2/3}\right]\left\{\left(\frac{-1}{3}\right)\left[UF_0^{-1/3}z^{1/3}\right]\right.$$
$$\left.-\eta\frac{\mathrm{d}}{\mathrm{d}\eta}\left[UF_0^{-1/3}z^{1/3}\right]\right\}$$
$$-\left[\overline{u^2}F_0^{-2/3}z^{2/3}\right]\frac{\mathrm{d}}{\mathrm{d}\eta}\left[WF_0^{-1/3}z^{1/3}\right]$$
$$-\left[\overline{uw}F_0^{-2/3}z^{2/3}\right]\left\{\left(\frac{-1}{3}\right)\left[WF_0^{-1/3}z^{1/3}\right]\right.$$
$$\left.-\eta\frac{\mathrm{d}}{\mathrm{d}\eta}\left[WF_0^{-1/3}z^{1/3}\right]\right\}$$
$$+\left[g\beta\overline{w\theta}F_0^{-1}z^2\right]-\left[\Phi_{rz}F_0^{-1}z^2\right] \quad \text{(A5)}$$

Appendix B

The purpose of this appendix is to estimate the leading errors in the balances of the second moment equations and the corresponding uncertainty in the pressure correlation terms. First, we establish the dominant source of error in the mean flow equations since [3] measured all the terms of these equations. Then we use these to estimate how much error is introduced in the calculation of the dissipation rates, which are obtained in [3] by balancing the turbulence temperature variance and turbulence kinetic energy equations. After this we estimate the errors present in the second moment balances.

The transport equations for mean energy and mean-momentum equations are

$$U\frac{\partial}{\partial r}(g\beta\Delta\Theta)+W\frac{\partial}{\partial z}(g\beta\Delta\Theta)$$
$$=-\frac{1}{r}\frac{\partial}{\partial r}\left(rg\beta\overline{u\theta}\right)-\frac{\partial}{\partial z}\left(g\beta\overline{w\theta}\right) \quad \text{(B1)}$$

$$U\frac{\partial W}{\partial r}+W\frac{\partial W}{\partial z}$$
$$=-\frac{1}{r}\frac{\partial}{\partial r}(r\overline{uw})-\frac{\partial}{\partial z}\left(\overline{w^2}-\overline{u^2}\right)+g\beta\Delta\Theta \quad \text{(B2)}$$

Their balances are given in Ref. [3]. Since all the terms in these equations are measured, it is possible to calculate the error in these balances. This is also done in [3]. Since the mean quantities can be measured relatively accurately, it is safe to assume that this error is primarily due to the error in second moment terms. Therefore, we conclude that the dominant source of error formean energy equation is $-\frac{1}{r}\frac{\partial}{\partial r}(rg\beta\overline{u\theta})$ and for mean momentum equation it is $-\frac{1}{r}\frac{\partial}{r}(r\overline{uw})$. Now we go to the temperature variance equation to find out the uncertainty involved in obtaining its dissipation rate.

$$U\frac{\partial}{\partial r}\left(\frac{\overline{\theta^2}}{2}\right)+W\frac{\partial}{\partial z}\left(\frac{\overline{\theta^2}}{2}\right)=-\frac{1}{2}\left\{\frac{1}{r}\frac{\partial}{\partial r}r\left(\overline{u\theta^2}\right)+\frac{\partial}{\partial z}\left(\overline{w\theta^2}\right)\right\}$$
$$-\overline{u\theta}\frac{\partial}{\partial r}\Delta\Theta-\overline{w\theta}\frac{\partial}{\partial z}\Delta\Theta-\epsilon_\theta \quad \text{(B3)}$$

Its balance is presented in [3]. From this balance it is

found that theturbulent production $-\overline{u\theta}\Delta\Theta/\partial r$ and the thermal dissipation rate, ϵ_θ are the two largest terms. The thermal dissipation is obtained as the closing term in the balance. Obviously any errors present in the balance have beenlumped into the thermal dissipation term. We assume that most of the error in the balance is due to $-\overline{u\theta}\partial\Delta\Theta/\partial r$ and occurs through $\overline{u\theta}$. From the mean energy equation we already know the error involved in $\overline{u\theta}$ and we can estimate the error involved in obtaining ϵ_θ from the balance of above equation.

Same approach is used in calculating the error in the mechanical dissipation rate, ϵ, which is obtained from the balance of turbulence kinetic energy

$$U\frac{\partial}{\partial r}\left(\frac{\overline{q^2}}{2}\right)+W\frac{\partial}{\partial z}\left(\frac{\overline{q^2}}{2}\right)\approx-\frac{1}{2}\left\{\frac{1}{r}\frac{\partial}{\partial r}r\left(\overline{uq^2}-\frac{1}{5}\overline{uq^2}\right)+\frac{\partial}{\partial z}\left(\overline{wq^2}-\frac{1}{5}\overline{wq^2}\right)\right\}$$

$$-\overline{u^2}\left(\frac{\partial U}{\partial r}+\frac{U}{r}\right)-\overline{uw}\frac{\partial U}{\partial z}-\overline{uw}\frac{\partial W}{\partial r}-\overline{w^2}\frac{\partial W}{\partial z}$$

$$+g\beta\overline{w\theta}-\epsilon \tag{B4}$$

The approximation sign is used because the pressure diffusion term is estimated from a model $\overline{pu_i}=-\overline{q^2u_i}$ due to [2] (see [3] for details). However, the main error in this balance is due to the production term $-\overline{uw}\partial W/\partial r$. The error in $\overline{uw}$ is estimated from the error in the mean momentum equation balance.

Finally, we assume that to the first order the errors introduced in the heat flux balances are due to the errors in their production terms and those in the Reynolds stress balances are due to the errors in production and dissipation terms. These errors vary with the radial position but the maximum error occurs at about $r/z=0.08$. Therefore, the values of the error given below are for $r/z=0.08$. If we carry out these steps we find out that the maximum error in the thermal dissipation rate, ϵ_θ is 25%. The maximum error in the mechanical dissipation rate, ϵ, is 16%. This means that the uncertainty in the time scale ratio $\tau_r=\overline{q^2}\epsilon_\theta/\overline{\theta^2}\epsilon$ is about 8% (=1.25/1.16).

In the vertical heat flux balance the leading source of error is due to $-\overline{uw}\partial\Delta\Theta/\partial r-\overline{u\theta}\partial W/\partial r$ and as a result pressure correlation Π_z is underestimated by 18%. In the radial heat flux equation the leading source of error is due to $-\overline{uw}\partial\Delta\Theta/\partial z-\overline{u\theta}\partial U/\partial r$ and as a result pressure correlation Π_r is underestimated by 5%.

In the $\overline{w^2}$ equation the primary error is due to $-2\overline{uw}\partial W/\partial r-2\epsilon/3$. The $-2\overline{uw}\partial W/\partial r$ is underestimated by 21% whereas $-2\epsilon/3$ is underestimated by 15%. However, these errors offset each other with the net result that the pressure correlation Π_{zz} is underestimated by about 28%. Similarly, the Π_{rr} is underestimated by 20%. In $\overline{uw}$ equation there is no $-2\epsilon/3$ term. The error introduced by $-\overline{uw}(\partial U/\partial r+\partial W/\partial z)$ is negligible because $\partial U/\partial r$ and $\partial W/\partial z$ almost cancel each other out. (From continuity $\frac{1}{r}\frac{\partial rU}{\partial r}+\frac{\partial W}{\partial z}=0$.) In this case then the primary source of error is due to the diffusion term. However the approach used here does not allow us to calculate this error. As a rough estimate we can assume that the percent error in Φ_{rz} is the same as the percent error in Φ_{zz} i.e. Φ_{rz} is underestimated by 21%.

These errors are marked on Figs. 2 and 3. These errors imply that the levels of pressure correlations are higher than what is shown in figures. It should be noted that if error in the second moments and the dissipation rates is accounted for then the levels of pressure correlations from models will also be higher than what is shown in figures. However the relative difference between the experiment and model will approximately remain unchanged.

References

[1] B.E. Launder, G.J. Reece, W. Rodi, Progress in the developmentof a Reynolds stress turbulence closure, J. Fluid Mech 68 (1976) 537–566.

[2] J.L. Lumley, Computational turbulence modeling, Advances in Applied Mechanics 18 (1978) 123–176.

[3] A. Shabbir, W.K. George, Experiments on a round turbulent buoyant plume, J. Fluid Mech 275 (1994) 1–32.

[4] G.K. Batchelor, Heat convection and buoyancy effects in fluids, Quart. J. Royal Met. Soc 80 (1954) 339–358.

[5] W. Rodi, A new algebraic stress relation for calculating the Reynolds stresses, Z. Angew. Math. Mech 56 (1976) 219.

[6] G.R. Newman, B.E. Launder, J.L. Lumley, Modeling the behavior of homogeneous scalar turbulence, J. Fluid Mech 111 (1981) 217–232.

[7] C. Beguier, I. Dekeyser, B.E. Launder, Phys. Fluids 21 (1978) 307–310.

[8] J.L. Lumley, Pressure strain correlation, Phys. Fluids 18 (1975) 750.

[9] A.S. Monin, On symmetry properties of turbulence in the surface layer of air, Izv Akad Nauk, SSR, Fizika Atmosf 1 (1965) 45.

[10] O. Zeman, J.L. Lumley, Modeling buoyancy driven mixed layers, J. Atm. Sci 33 (1976) 1974–1988.

[11] O. Zeman, Progress in the modeling of planetary boundary layers, Anl. Rev. Fluid Mech 13 (1981) 253–272.

[12] S. Tavoularis, S. Corrsin, Experiments in nearly homogeneous turbulent shearflow with a uniform mean temperature gradient, J. Fluid Mech 104 (1981) 311–348.

[13] B.E. Launder, Heat and mass transport, in: Bradshaw (Ed.), Turbulence, Springer-Verlag, Berlin, 1976, pp. 231–287.

[14] P.J. Morris, Modeling of the pressure redistribution terms, Phys. Fluids 27 (1984) 1620.

[15] D.B. Taulbee, J.R. Sonnenmeier, K.M. Wall, Stress relation for three dimensional flows, Phys. Fluids 6 (1994) 1399.